

<https://doi.org/10.18524/1810-4215.2025.38.341022>

## JUPITER'S DAM RADIO EMISSION AND SOLAR ACTIVITY: IO-DEPENDENT AND NON-IO SOURCES

N. O. Tsvyk

Institute of Radio Astronomy of the NAS of Ukraine, Kharkiv, Ukraine  
*natalitsv69@gmail.com*

**ABSTRACT.** We study Jupiter's DAM radio storms to identify the features that may correlate with solar wind and coronal mass ejections (CME). We investigate the dynamics of DAM storms and burst features, and explain them by considering MHD processes associated with Io and the presence of gas in Jupiter's lower magnetosphere.

DAM radio storms occur when plasma injected by Io or by solar wind propagating along Jupiter's magnetic field lines into the auroral zone of Jupiter's lower magnetosphere together with low-frequency Alfvén wave. Those MHD oscillations in low magnetosphere can trigger ionization processes and create streamers, activating maser instabilities in the electron plasma. This can occur under the influence of dense solar wind and CME that penetrate to Jupiter's magnetosphere, creating high-latitude currents with non-Io radio storms, and enhancing Io-dependent sources of DAM radio emissions.

We found that dynamics of development of Io-dependent and non-Io DAM radio storms have similar features and evolutionary peculiarities. That time periodicities (5 min and 20 min durations) may be connected with MHD instabilities activated by Io, that modulate the current sheets system in all auroral zone. The power of Io-dependent storms is modulated by the solar wind pressure on the magnetosphere of Jupiter. On the other hand, in non-Io radio sources associated with solar plasma injections, due to the content of high-energy ions which scatter on the gas fluids, a number of specific radio bursts are formed, for example, having zebra structures on high-resolution dynamic spectra.

**Keywords:** DAM radio emission, Alfvén waves, magnetosphere, solar wind, Jupiter.

**АННОТАЦІЯ.** В цій роботі буде вивчено декаметрові (ДКМ) радіобури Юпітера, для того, щоб виявити особливості, які можуть бути пов'язані із впливом сонячного вітру та корональних викидів маси (CME) на утворення радіобур та сплесків ДКМ радіо випромінювання. Ми розглядаємо динаміку бур та особливості окремих ДКМ сплесків, та пояснюємо їх з урахуванням МГД процесів, пов'язаних з Io, та процесів, що відбуваються за наявності нейтрального газу в нижній магнітосфері Юпітера.

Вважаємо, що бури ДКМ радіовипромінювання виникають, коли плазма, інжектована на Io, або плазма сонячного вітру проникає до авроральної зони нижньої магнітосфери Юпітера, поширюючись вздовж ліній магнітного поля Юпітера разом з альвенівськими хви

лями низької частоти. Ці МГД коливання в нижній магнітосфері можуть запускати процеси іонізації плазми і формувати стримери, та будуть активувати Мазерні нестійкості на електронах. Під впливом щільного сонячного вітру і корональних викидів маси змінюється структура магнітосфери Юпітера, з'являється високоширотні плазмові течії, дотичні до появи не-Io ДКМ штормів, та посилюється ДКМ радіовипромінювання, яке контролюється Io.

Враховано, що динаміка розвитку ДКМ радіобур, залежних від Io та незалежних від Io, мають схожі риси та еволюційні особливості. Так, їх спільні періодичності у часі (5 хвилин та 20 хвилин тривалості) можуть бути пов'язаними з МГД нестійкостями, активованими Io, які модулюють систему струмових шарів у всій авроральній зоні. Потужність бур, залежних від Io, модулюється динамічним тиском сонячного вітру на магнітосферу Юпітера. З іншого боку, в радіоджералах незалежних від Io, і пов'язаних з інжекціями сонячної плазми, завдяки вмісту високоенергетичних іонів, що стикаються з газовим середовищем, формується ряд специфічних радіо сплесків, наприклад, такі, що мають зебра-структурі на динамічних спектрах високої роздільної здатності.

**Ключові слова:** ДКМ радіовипромінювання, альвенівські хвилі, магнітосфера, сонячний вітер, Юпітер.

### 1. Introduction: the Io-dependent and non-Io sources observed in DAM radio storms

Jupiter's DAM radio storms were observed in radio telescopes in Ukraine, France, USA (Florida) and others (see: Ryabov & Gerasimova, 1990; Ryabov, 2001; Ryabov et al 2014; Marques et al., 2017; Flagg et al., 1991), as well as during the mission's observation by Voyager-1,2, Juno and others (e.g., see: Genova, 1985; Barrow et al., 1986; Liu et al., 2021) on time-scale of low resolution (hour, min, second) and high resolution (millisecond scale). In Ukraine such observations have been made at the UTR-2 and URAN-4 telescopes. We can see on them the different types of sources: dusk-side (A, C) sources and down-side (B, D) sources, for Io-dependent and non-Io sources. We also made and presented in Table 1 a comparison of the observed properties of these dynamic spectra for DAM storms (on a large scale and with higher resolution), such as storm evolution, temporal and frequency modulation of the burst pattern, observed high-resolution features of the dynamic spectrum in DAM bursts using UTR-2 and URAN-4 data and a thorough analysis of data from a telescope in France, which was carried out by Marques et al. (2017).

Table 1: Compare of Io-dependent and non-Io storms

	<i>Io-dependent sources</i>	<i>Non-Io-storms</i>
Arcs forms	Dusk Io-A,C: „late” arcs Down Io-B,D: „early” arcs	Dusk non-Io-A,C: „late” arcs Down non-Io-B,D: „early” arcs
Storm duration	50 min – 1.5 hr A number of Dusk storm cases are grater then in Down cases	40 min – 1.2 hr A number of the storms cases are grater then in Io-dependend storm cases
Position: $\lambda_{CML}$ and $\lambda_S$	$\lambda_{CML} \sim 240^\circ \pm 40^\circ$ (Io-A); $\sim 140^\circ \pm 40^\circ$ (Io-B); $\sim 320^\circ \pm 40^\circ$ (Io-C); $\sim 125^\circ \pm 90^\circ$ (Io-D). ( $\lambda_S + 30^\circ$ ) $\sim \Lambda_{Io} \sim 195^\circ \pm 80^\circ$ (Io-A,B)	$\lambda_{CML} \sim 80-190^\circ$ (non-Io B); $\sim 200-340^\circ$ (non-Io A, C); $\lambda_{CML} \sim 60-320^\circ$ (non-Io D)
Intensity	The intensity Io- and non-Io storms are compared; have the finest bursts	Non-Io storms have some much power, and some less durations
Max-frequency	Io-A,B (N-sph.): 39 MHz; Io-C,D (S-sph.): 27 MHz	Non-Io: up to 28 MHz
Polarization	Io-A,B (N-sph.): RH dominated; Io-C,D (S-sph.): LH dominated	(N-sph.): RH dominated; (S-sph.): LH dominated
UV, IR	UV, IR brightness in N-pole oval is grater then in S-pole	UV spots observed in auroral zones. A number of UV spots are grater at N-pole then at S-pole
Solar wind	A number of storm cases and storm power depends on SW kinetic power	A number of storm cases increase with solar wind kinetic power

We are interested in what are the common properties and differences in the dynamic spectra, in order to explain the mechanism of activation of Jupiter's DAM radio emission, and they possible connection with Solar wind ejections. So, we see such main periodicities for Io-dependent sources: the storm duration of 1-3 hr, the periodicity of 20-40 min with arcs structure (be seen the early-arc modulation for Down sources, and the late-arcs for Dusk sources); and the periodicity of 5 min of common cases of storm spectrum (see: Dessler & Hill, 1979; Ryabov, 2001; Marques et al., 2017). In addition, we see the lanes modulation ( $\sim 0.1$ -1 MHz), and in the dynamical spectra of high resolution there is the L- or S-bursts with slow or fast drift; and with periodicity of about 1s for L-bursts, and of 0.1s, 0.03s, 0.003-0.01s for S-bursts (see: Flagg et al., 1991; Ryabov & Gerasimova 1990; Ryabov, 2001; Ryabov et al., 2014).

Many models of the Io correlation mechanism propose that the 5-minute modulations are associated with Io-generated Alfvén waves with a 10-minute period, which further activate DAM bursts with fast S-drift in the dynamical spectra (see: Su et al., 2006; Hess et al., 2007). However, only in Io-dependent storms we registry the many fine structures of S-bursts in the dynamic spectrum, together with L- and Narrow-band bursts. These storms also correlate with infrared and far-ultraviolet data obtained with the Hubble Space Telescope (Gerard et al., 2014). The Io flux tube draws a main oval in the Jupiter's surface, which corresponds to the locations where Io-dependent radio sources radiate. Considering a pole tilt, a region with maximum magnetic fields is formed at  $\lambda_{CML} \sim 165^\circ$  for N and at  $\sim 240^\circ$  for S-hemisphere, which is responsible for the maximum number of DAM storm occurrences with  $(\lambda_S + 30^\circ) \sim \Lambda_{Io} \sim 195^\circ$  (Marques et al., 2017).

Similar periodicities we can also observe in the non-Io storms, for example, we observe storms with duration of about  $\sim 1$  hr, and we see modulation with periods of 5 minutes within the arc structures of 20-30 minutes duration (Barrow et al., 1986; Marques et al., 2017). In high-resolution dynamic spectra, we most often observe L-bursts, or in some rare cases, we observe Zebra-type and Narrow-band bursts (Ryabov & Gerasimova, 1990; Marques et al., 2017; Panchenko et al., 2018). The fact of similar modulation with 5-minute periods in non-Io sources is unexpected.

On the other hand, high-latitude non-Io storms can be activated directly by the solar wind. So, Barrow et al. (1986) find from Voyager-1 data that correlation of DAM storms with solar wind kinetic power of  $P_{SW} \sim (m_p n_{ei} v_{sw}^2)$ , and a number of that storm cases is increased when solar wind fluctuation and CME reach the Jupiter's magnetosphere. Incidentally, Barrow et al. found that the correlation with the solar wind works for both non-Io and Io-dependent storms. This fact convinces us to search a general mechanism to explain these types of low-frequency modulations in the DAM radiation of Io-dependent and non-Io storms. How this mechanism works in the Jupiter magnetosphere and how the solar wind affects the DAM radio emission will be seen below.

## 2. The activation mechanism for Jupiter DAM Radio Emission in Io-dependent sources

### 2.1. Io-Jupiter interaction

The Io-dependent DAM radio storms of Jupiter are associated with the satellite Io, which generates Alfvén waves (with a period of  $\sim 10$  minutes) in the region of Jupiter's

magnetosphere with a strong magnetic field, under the influence of which the "rotational energy" of Jupiter is converted into DAM radio energy and non-thermal acceleration of plasma particles.

This Io – Jupiter interaction mechanism have been proposed and developed by Gold-reich &Lynden-Bell, (1969), Dessler &Hill, (1979), Su, et al. (2006), Hess, et al. (2007), and others. They studied how the Alfvén wave is generated and transported from Io, and how it interacts with Jupiter's lower magnetosphere, which consists of plasma and gas fluids.

The plasma density in the auroral zones is very low, so the active plasma is mainly injected into the DAM sources from Io torus, transported along the Io-Jupiter flux tube into this zone with electric currents (see Su, et al. 2006, Hess, et al. 2007). Moreover, since this zone contains high-density neutral gas fluids, ionization can begin under the influence of low-frequency Alfvén waves generated by Io, which also adds plasma particles to these zones (see Boev, et al. 2001, Boev, 2005; Tsvyk, 2019, 2023, 2024). All these processes lead to the emergence of Io-dependent DAM radiation sources with S- and L-bursts.

The plasma in Io's torus is forced into co-rotation with Jupiter, meaning to share the same period of rotation. The Io torus fundamentally alters the dynamics of the Jovian magnetosphere when Io moves through the magnetosphere, and it generates the Alfvén wave electric fields of with periods of  $T_{A0} \sim 10$  min, which may be connected with the torus curvature and depend on how that Alfvén instability works.

The Alfvén wave pattern is formed in the magnetosphere by the interaction of Io and Jupiter, when Alfvén energy is transported to Jupiter along magnetic field lines and this involve the Io-torus plasma to move along the flux tube. The Alfvén waves are directed almost along the lines of Jupiter's rotation (along the torus), so Alfvén waves and Io-torus fluid are transported both to and away from Jupiter (into the outer magnetosphere) when the wave-vector  $k_A$  rotates in a period of 20-40 min. Thus, the current sheets and a magnetic disk have being formed in Jupiter's magnetosphere, sharing it into tubes or sheets with a width of  $2R_{\text{tor}} \sim 6 R_{\text{Io}} \sim 0.15 R_j$ , and Alfvén waves may transform to kinetic modes.

## 2.2. MHD waves in Io vicinity

Let us consider in a vicinity of Io the plasma and MHD wave parameters corresponding to a plasma torus. So, these are:  $n_{ei} \sim 200 \text{ cm}^{-3}$ ;  $T_{ei} \sim 10^5 \text{--} 10^6 \text{ K}$  (very dense and hot plasma, see: Krupp et al. 2004, Su et al. 2006), and this gives us:  $c_{Afx} \sim v_{ti} \sim 5 \cdot 10^4 \text{ m/s}$ ;  $v_{te} \sim 3 \cdot 10^6 \text{ m/s} = 0.01 c$  ( $c_{Afx} < v_{te} < c_A$ ). Such MHD instabilities, due to the rotation of Io in a strong magnetic field, generate the low-frequency (LF) Alfvén waves with a period of  $T_{A0} \sim 600 \text{ s}$  ( $k_A = 2\pi/\lambda_A$ ); the Alfvén velocity on the orbit of Io ( $z_j \sim 6$ ,  $\varphi \sim 0$ ) is:  $c_A \sim 0.25 \text{ c}$  ( $z_j$  in  $R_j$  units). Therefore, this velocity corresponds to the transfer of wave energy along the magnetic field lines from Io (at  $z_j \sim 5$ ) to the mirror point in the ionosphere ( $z_j \sim 0.014$ ), which lasts of  $\sim 7 \text{ s}$  by time.

The model parameters of Alfvén waves are represented in Table 2. So, using the typical MHD theory (see: Akhiezer, et al 1974, Kadomtsev, 1988), we find the following magnetic and electric fields for these Alfvén waves:  $B_{\omega y} \propto \xi_{\perp} k_{Az} B_{0z}$ ,  $E_{\omega z} \propto \omega (k_{Ax} c)^{-1} B_{\omega y}$ , with oscillations of  $\propto \exp(ik_A r -$

$i\omega t$ ). The wave's current is:  $j_z = e n_{ei} (v_{iz} - v_{ez}) \propto ik_A B_{\omega y}$  with phase shifted oscillations. For Alfvén modes with  $k_A$  directed almost along the rotation lines (in  $x$ -axis of perpendicularly to  $B_{0z}$ -magnetic lines,  $\theta_{kB} \approx 0.4995\pi$ ) the phase velocities are:  $c_{Afx} = c_A \cos^2 \theta_{kB} \approx 20 \text{ m/s}$  (along magnetic field), and  $c_{Afx} = c_A \cos \theta_{kB} \sin \theta_{kB} \approx 10^4 \text{ m/s}$  (nearly along  $k_A$ ). Therefore, those Alfvén wavelengths are:  $\lambda_A = T_{A0} c_A \cos \theta_{kB}$  and  $\lambda_{Az} = T_{A0} c_A$ .

## 2.3. A transport of MHD waves

The Alfvén wave velocity  $c_A$  depends on  $n_e(z_j)$  and  $B_{0z}(z_j, \phi)$  and varies along the magnetic field lines. It is specified as  $n_e(z_j)$  in the model of like Su, et al. (2006) (see Fig. 1), and we have chosen the dipole approximation for the Jupiter's magnetic field,  $B_{0z}(z_j, \phi) \approx 10 \text{ G} (1 + 3 \sin^2 \phi)(1 + z_j)^{-3}$  (as for N-pole at  $\lambda_{CML} \sim 165^\circ$ ), where  $z_j$  is the altitude from the Jupiter's surface (in  $R_j$  units) and  $\phi$  is the azimuthal angle of the observed point.

The plasma density at the foot of Io flux tube may increase from 0 to  $10^3 \text{--} 10^4 \text{ cm}^{-3}$  as the Io-related magnetic field lines move above the aurora zone, and the Io-plasma flows and are transported with Alfvén waves to the Jupiter surface along the magnetic field lines. Then, the presence of neutral gas fluids at the lower altitudes in the Jupiter magnetosphere leads to the low-frequency (LF) Alfvén wave velocity decrease from  $c_A$  to  $c_{ALF}$  because the neutral gas particles move together with the plasma oscillations through particle

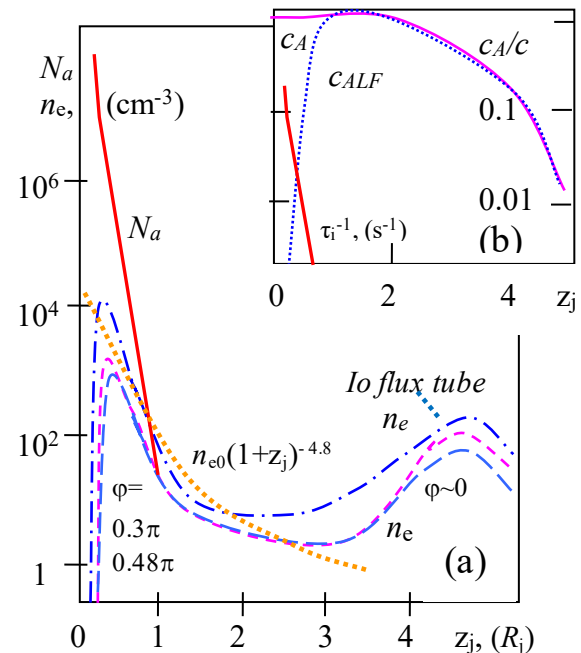


Figure 1: (a) The models for plasma  $n_e$  and gas  $N_a$  density variation at Jupiter magnetosphere along flux tube (altitudes  $z_j$  in Jupiter radius units). Curves are correspondent to the model like Su, et al. (2006) for Io flux tube and for other flux tubes at  $\varphi=0.48\pi$  and  $\varphi=0.3\pi$ . (b) The dependence of  $\tau_i$  time-scattering and  $c_A(z_j)$  velocities along Io flux tube for HF and LF Alfvén waves

Table 2: The Alfvén wave model parameters at the Io orbit and at the foot of Io-Jupiter flux tube. Here we take:  $B_{0z}$ ,  $k_A = (k_{AX}, k_{AZ})$ ; and  $k_{AX}^2 = k_{AX}^2 + k_{AY}^2 \approx k_{AX}^2$ .

	$z_j=5$ (Io orbit)	$z_j=0.5$	$z_j=0.3$ (atmosphere influence)
$c_A/c$	0.25	0.95	0.25
$c_{Afx}$	$4 \cdot 10^{-5} c$	$5 \cdot 10^3$ m/s	$5 \cdot 10^3$ m/s
$c_{Afz}$	20 m/s	1 m/s	5 m/s
$\theta_{kB}$	$0.4995\pi$	$0.49995\pi$	$0.4998\pi$
Wave length:	$\lambda_A$	$k_A, \text{m}^{-1}$	$\lambda_A/R_j$
$\lambda_A$	$4 R_{io} = 0.1 R_j$	$10^{-6}$	0.04
$\lambda_{AZ}$	$\sim 62 R_j$	$10^{-9}$	2000
$\lambda_{AX}$	$0.1 R_j$	$10^{-6}$	0.04
$\lambda_{AY}$	$0.13 R_j$	$7 \cdot 10^{-7}$	0.06
$\lambda_{Ax}$	$4 R_{io} = 0.15 R_j$	$6 \cdot 10^{-7}$	0.05
			$\lambda_A/R_j$
			$k_A, \text{m}^{-1}$

collisions on LF Alfvén waves (see Tsvykh, 2023, 2024; and considering the equations for low-ionized plasma by Smirnov, 1995, Kadomtsev, 1963, Braginsky, 1963, Akhiezer, et al. 1974):

$$c_A^2 \cong B_0^2 / (4\pi n_i m_p), \omega > \tau_{ia}^{-1},$$

$$c_{A\_LF}^2 \cong B_0^2 / (4\pi N_a m_p), \omega \ll \tau_{ia}^{-1}.$$

Here  $\tau_{ia}$  is the ion scattering time in the presence of a neutral gas:

$$\tau_{ia} \cong 1 / (v_{Ti} N_a a_\lambda^2) \approx 10^{14} \text{ cm}^{-2} / (v_{Ti} N_a).$$

Alternatively, high-frequency (HF) Alfvén waves move with  $c_A$ -velocity, and they velocity reaches the light speed at low ionosphere altitudes ( $z_j \rightarrow 0.014$ , in  $R_j$  units) where the plasma density comes to Zero. At these altitudes the gas temperature is about  $T_a \sim 1000$  K, and the ionization processes can occur at higher altitudes, while the ion particles cool and recombine lower down. Ionization occurs mainly through collisions of high-energy particles with gaseous fluids, and to a lesser extent through the impact of energetic photons of solar radiation. Thus, in the lower magnetosphere of Jupiter at  $z_j < 0.5$  we have  $T_a \sim 500$  K for gaseous particles, the ep-temperature is  $T_e > T_p \sim 2000$  K, and here is the zone where DAM radio sources have been activated above the auroral zones (see: Boev, et al. 2001, Boev, 2005, Withers & Vogt, 2017).

Figure 1 shows the density variations for and outside the Io flux tube, using a model similar to Su et al. (2006), where  $N_a$  is the gas density and  $n_e$  is the plasma density ( $n_e \approx n_p$ , as well as some other impurity ions). And Fig. 1b shows the variation of  $c_A$  in the lower magnetosphere of Jupiter for HF and LF Alfvén waves. Thus, the ion-atom collision frequency began to affect the MHD waves at heights  $z_j < 0.5$ , where the atmospheric density is much higher than the plasma density.

#### 2.4. MHD waves in lower magnetosphere and DAM storms

Now we can calculate the Alfvén wave parameters at ( $z_j \sim 0.5, \varphi \sim \pi/3$ ) using these magnetosphere data. The Alfvén velocity here is high,  $c_A \rightarrow c$ , and corresponds to the fast transfer of MHD energy along the magnetic field lines. The phase velocity for Alfvén wave-modes ( $T_{A0}$ ) with  $\theta_{kB} \sim 0.49995\pi$  is:  $c_{Afz} < 1$  m/s;  $c_{Afx} \sim 5 \cdot 10^3$  m/s. The current sheets shrink adiabatically because the  $B_0$ -magnetic field lines are focused at small  $z_j$  as in the dipole model:  $\lambda_{Ax} = \lambda_{Ax0} (1+z_j)/6$ . The plasma parameters in this zones are:  $n_{ei} \sim (30-10^4) \text{ cm}^{-3}$ ;  $T_{ei} \sim 3000$  K, that is give us:  $c_{Afx} \sim v_{ti} \sim 4 \cdot 10^3$  m/s;  $v_{te} \sim 2 \cdot 10^5$  m/s  $\sim 0.001 c$  ( $c_{Afx} < v_{te} < c_A$ ). The magnetic field lines  $B_{0z}$  are curved as (dipole model); and the current sheets can be tilted towards the magnetic field lines under the of Jupiter's plasma rotation or by the influence of fast magneto sound (MS) waves, which are transported at a speed of  $c_A$  and have large length  $\lambda_{fms} > 6 R_j$  at  $T_{A0}$  wave-period.

At lower altitudes, e.g., at ( $z_j \sim 0.3$  and  $\varphi \sim \pi/3$ ), it is necessary to take into account the presence of high-density neutral gas for the LF Alfvén wave, and we have its velocity of  $c_{ALF} \sim 0.025c$ , which corresponds to the anomalous increase in the Alfvén energy flux at  $z_j \rightarrow 0$ . And we get the following phase velocity of Alfvén  $T_{A0}$ -modes (with  $\theta_{kB} \sim 0.4998\pi$ ):  $c_{Afz} \sim 3$  m/s;  $c_{Afx} \sim 5 \cdot 10^3$  m/s, where the current sheets are compressed adiabatically in the  $x$  direction due to the coincidence of magnetic field lines at  $z_j \rightarrow 0$ .

The plasma parameters in this zone are:  $n_{ei} \sim (1-10^4) \text{ cm}^{-3}$ ;  $T_{ei} \sim 3000$  K, so we have:  $c_{Afx} \sim v_{ti} \sim 4 \cdot 10^3$  m/s; and  $v_{te} \sim 2 \cdot 10^5$  m/s  $\sim 0.001 c$ . The MHD power (or wave energy density) increases with decreasing wave speed  $c_A$ , and when  $c_A \rightarrow c_{ALF}$  (at  $z_j \rightarrow 0$ ), this gives us a power increase of  $> 100$  factor compared to the MHD energy density at  $z_j = 5$ . In the Io-dependent DAM sources this effect leads to the strong plasma hitting which lead to the ionization begins at the wave-mirror point. In addition, the fast MS waves can affect to the current sheets at this mirror point, and the streamer-like structures appear in each of current sheet regions.

All these processes lead to the streamer-like stratification of the lower magnetosphere by MHD waves, and here the DAM radiation is activated with the observed bursts and modulation features which are presented in Table 3.

Table 3: *L* and *S* bursts: time periodicities and the storm shape in dynamical spectrum

Io-dependent storms	5 min, 20 min, arc-shaped structure	Alfven waves by Io generated: $T_{A0} \sim 10$ min. Due to $k_A$ rotates and Io-plasma injection: $T_{\text{storm}} \sim 20$ min. The arcs correspond to the geometry of the Io – Jupiter flux tubes, where the plasma fluids move to Jupiter
L-bursts	1 s	This period may be associated with the $\tau_i$ -time scattering for ions with atoms of neutral gas in the lower magnetosphere
S-bursts (Io-dependent source)	0.002-0.01 s (with fast drift)	They may be connected with start of the ionization process, refraction process, so as connected with burst modulation of HF-Alfven waves within the streamers ( $T_{A1} \sim 0.005-0.01$ s, $T_{A2} \sim 0.03-0.1$ s). They may be generated in the wave-mirror points at the Jupiter surface.
N-bursts	0.5-1 MHz (in bands)	They are associated with modulation of the plasma density, and the shape of the spectra is obtained due to refraction effects inside the DAM sources.
Bursts in non-Io storms	0.1-1s; 0.01 s (in 0.5 MHz bands)	They have a shorter duration and lower intensity. These bursts have dominantly L-shaped bursts, but in rare cases it appears zebra bursts with fine periodicity, $\sim 0.01$ s

### 3. Jupiter DAM radio emission of non-Io sources: a role of Solar wind and CME

We now consider the structure of Jupiter's magnetosphere, the role of Io in modulating the magnetic disk, and the influence of the solar wind on the activation of non-Io DAM radio sources in high-latitude auroral zones. We note that the activation of DAM sources requires the presence of plasma fluid in the auroral zone, and the Maser radiation mechanism arise due to the Alfvén waves working in current sheets.

So, when the solar wind (SW) interacts with Jupiter's magnetosphere, which has a strong magnetic field, a structure of bow shock – tail emerges in this magnetosphere (see: Khurana et al. 2004). Then, when the SW-pressure increases or a coronal mass ejection (CME) reaches Jupiter, the magnetic field reconnection occurs within the bow shock wave, or in the tail of Jupiter's magnetosphere at a distance of  $z_j \sim 15$ , and solar plasma penetrates into Jupiter's auroral zones. We now consider the effects in solar wind turbulence on Jupiter's magnetosphere, leading to current reconstructions and tail fluctuations. We then review how these processes activate the non-Io DAM sources in Jupiter's high-latitude magnetosphere (e.g., for Ganymede-dependent DAM sources and others). We conclude this review by examining a number of special DAM bursts in non-Io storms (such as zebra pattern bursts) that can occur in the presence of solar wind plasma.

The feature of Jupiter's magnetosphere is a complex dynamical system of current sheets that are created in its various regions. In the tail of Jupiter's magnetosphere, a magneto-disk arises, consisting of a direct current and others, which may rebuild due to the pressure of Solar wind plasma that coming into Jupiter's magnetosphere. Thus, according to the Juno mission, several current sheets were observed in the magneto-disk region, which were located in the plane of Jupiter's equator with a diameter of  $20 R_j$  and extended to a distance of  $z_j > 20$  (see: Liu et al., 2021). Then, this magneto-disk is stratified into radial elongated sheets with Io-correlated periods of  $T_{A0} \approx 10$  min. The Juno mission also recorded the relativistic plasma particles with energies of 10-1000 keV

( $\propto \varepsilon^{-2.3}$ ), which may be accelerated due to particle scattering on MHD-current sheets of been generated by Io.

Figure 2 presents the pressure dependences in Jupiter's magnetosphere, which vary in the range  $z_j = 0.1-100$  and are approximated using spacecraffts data and models of Sentman et al. (1975), Khurana et al. (2004), Su et al. (2006). So, the solar wind plasma may penetrate to the Io torus, where we have the presser equilibrium of  $P_{ei} \sim P_{SW}$ , and thus the Io – solar wind interaction will control a “machine” of Alfvén wave productions.

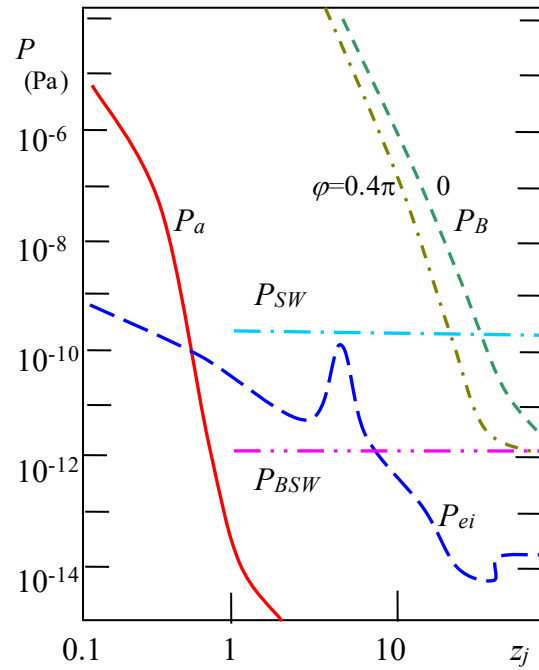


Figure 2: The models of presser variations in Jupiter magnetosphere. Here:  $P_B$  is Jupiter's magnetic field presser,  $P_a$  is the neutral gas presser,  $P_{ei}$  is the ep-plasma presser (with impurities of other ions); and they are comparison with typical solar wind dynamical ( $P_{sw}$ ) and magnetic ( $P_{BSW}$ ) pressers.

Firstly, the energetic SW plasma particles are frozen into the interplanetary magnetic field, and they penetrate through the bow shock to Jupiter's magnetosphere, which has a strong magnetic field that co-rotates with the planet. SW parameters at Jupiter's orbit (5 a.u.) are:  $n_{ei} \sim 1 \text{ cm}^{-3}$ ;  $v_{ei} \sim 280 \text{ km/s}$ ;  $B_{sw} \sim 10^{-5} \text{ G}$ ;  $T_e \sim 10 \text{ K}$ ;  $T_i \sim 10^5 \text{ K}$  for a slow wind, and  $n_{ei} \sim 0.4 \text{ cm}^{-3}$ ;  $v_{ei} \sim 600 \text{ km/s}$ ;  $B_{sw} \sim 10^{-5} \text{ G}$ ;  $T_i \sim T_e \sim 10^5 \text{ K}$ , for a fast wind, correspondently. The bow shock temperature is about  $T_e > T_i \sim 10^5 \text{ K}$ , and magnetosphere parameters at  $z_j$ -distances in the tail region may be chosen:  $n_{ei} \sim 0.3 \text{ cm}^{-3}$ ;  $v_{cor} \sim 200\eta \text{ km/s}$  (carries co-rotation velocity, where  $\eta > 5$ );  $B_{0j} \sim 4.5 \cdot 10^{-3} \text{ G}$  – for  $z_j = 15$ ;  $n_{ei} \sim 0.005 \text{ cm}^{-3}$ ;  $v_{cor} \sim 640\eta \text{ km/s}$ ;  $B_{0j} \sim 0.6 \cdot 10^{-3} \text{ G}$  – for  $z_j = 50$ ; and  $n_{ei} \sim 0.02 \text{ cm}^{-3}$ ;  $v_{cor} \sim 1200\eta \text{ km/s}$ ;  $B_{0j} \sim 0.3 \cdot 10^{-3} \text{ G}$  – for  $z_j = 100$ .

The SW fluxes with density fluctuation are transported and have the transformation by that way: firstly, from intra-planetary space into the Jupiter's bow shock ( $z_j \sim 50$ ); then, to the magnetopause ( $z_j < 40$ , or trapped to the magneto-tail); to the magneto-disk ( $z_j \sim 15$ , are in current sheets that transforms to the direct current); and to the return current (from  $z_j \sim 15$  to  $z_j \sim 5$ ); and finally they arrive to the auroral zones in the Jupiter's lower magnetosphere ( $z_j < 0.5$ ,  $\varphi \approx 0.3..0.5 \pi$ ). The time of this transport is estimated to be about 10 hours or more, when solar particles move with diffusion and flux compression in the form of a hot non-thermal plasma flow ( $T_{ei} > 10^5 \text{ K}$ ) with a velocity of about  $v_{tr} \approx 3 \cdot 10^4 \text{ m/s}$ , which is approximately equal to the Jupiter's co-rotation velocity with its magnetic field, in which the plasma particles are frozen.

At the reconnection point in Ganymede's orbit ( $z_j \sim 15$ ), electric field and current instabilities arise when the Alfvén theorem is breakdown in this region,  $\frac{\partial E}{c \partial t} = \text{rot} B - \frac{4\pi}{c} j$ . Thus, due to a strong fluctuation of the electric field, the Alfvén waves are generated along the magnetic field lines in the direction to Jupiter and in the direction of a radial current, respectively, forming a reverse current with new current sheets and the plasmoid ejections to magnetosphere tail. So, the reverse currents passing through the Io torus zone are modulated by its current sheets, and the solar fluids are transported to the auroral zone of Jupiter, being compressed by a factor of  $(z_j + 1)/15$ . Thus, under the influence of the magnetic disk, we observe the duration of the DAM source activity of  $\sim 20\text{--}40$  minutes in non-Io storms, the same as in Io-dependent sources.

Let we analyze now the non-Io DAM storm with Zebra-pattern bursts which was observed in URAN data by Panchenko, et al. (2018), to compare them with the zebra-like dynamical spectrum in the Io-C sources (storm at 8.09.1999, see: Ryabov, 2001). So, both non-Io and Io-C radio sources with zebra-bursts may be associated with ion plasma density fluctuation. For non-Io sources, these oscillations develop in the presence of high-density solar plasma with high-energy ions. Instead, for Io C sources, plasma fluctuations occur at the altitude where the plasma coming from Io interacts with the neutral gas of Jupiter's ionosphere.

So, if we observe a non-Io radio source when the solar plasma flux reaches Jupiter at  $z_j \sim 0.1$  and has a fluid compressed by  $(0.01\text{--}0.1) (50/(1+z_j))^2 \approx (20\text{--}200)$  times, then we can estimate the plasma density in this radio source as:  $200 n_{sw} < 10^3 \text{ cm}^{-3}$ . In the work of Panchenko et al. (2018), the emergence of Zebra-like spectra with observed

frequency oscillations  $\Delta f \approx 0.3\text{--}1.5 \text{ MHz}$  in non-Io sources is explained by the resonance between ion cyclotron and electron plasma oscillations:  $f_{pi} = s f_{bi} \approx 0.5 \text{ MHz}$  ( $s = 5..10$ ), where  $f_{bi} \approx 0.01 \text{ MHz}$ , and this is explained by the plasma density  $n_i \approx 10^4 \text{ cm}^{-3}$ . Therefore, this plasma density is very high for the SW fluid entering these sources. The other way, taking account an neutral gas influence into the SW plasma flux, that Zebra-like pattern can be explained also as the high-energy ions fluctuation in some LF-MHD waves, of  $T_A \approx 1 \text{ s}$  periods and  $c_{ALF}/c \approx 10^{-3}$ , taking account that scatter time of  $\tau_{ia\_sw} \sim 0.03 \ll \tau_{ia}$  for that SW-ions, that give us to  $\Delta f_{be} \sim 0.5 \text{ MHz}$  fluctuation in altitude  $z_j \sim 0.1$ :

$$\lambda_{ZA \text{ LF}} \sim \lambda_{Z \text{ FMS LF}} \approx c_{ALF} T_A \approx 0.01 R_j.$$

#### 4. Conclusions

Both the Io-dependent and the non-Io DAM radio storms have similar time variation in the dynamical spectrum and shape structure, which is connected with current sheets that produced by Io in Jupiter magnetosphere.

To activate the Jupiter's DAM radio emission, both the presence of plasma in the lower magnetosphere and low-frequency Alfvén waves are necessary, which can support the mechanism for generating DAM radiation and their bursts (for example, due to the maser cyclotron instability).

The presence of plasma fluids within the magnetosphere help to save the magnetic rotation moments over large distances in Jupiter's magnetosphere. The same way, the plasma supports the processes of rotation moments exchange between Jupiter and its satellites. The atmosphere in the lower magnetosphere concentrates the energy of Alfvén waves and helps to convert it into the DAM radio emission. Then, LF-Alfvén waves arising due to the Io rotation lead to the streamer formations.

The Alfvén waves generated by Io-Jupiter interaction convert the MHD energy into radio bursts, and produce the current sheets. The fast MS wave makes small changes to the structure of current sheet, may support the streamer formation, but they are insignificant in main storm structure.

Solar wind fluctuations and CMEs add the plasma fluids to the outer region of Jupiter's magnetosphere, and they produce the changes in current sheets due to the magnetic fields reconnection. Thus, the solar wind can influence the DAM radio emission by maintaining the MHD instabilities in the lower magnetosphere, and producing the non-Io DAM radio sources.

*Acknowledgements.* This work was carried out with the support of STCU "Crown" project No.6435.

#### References

- Akhiezer A.I., et al.: 1974, *Plasma electrodynamics* (in Russian), 719. – Nauka, Gl. red. phys.-mat. Literatury/eds. Akhiezer A.I., Moscow.
- Barrow C. H., Desch M.D., Genova F.: 1986, *A&A*, **165**, 244.
- Behannon K. W., Burlaga L. F., Ness N. F.: 1981, *JGR*, **86**, A10, 8385-8401.
- Boev A.G., Udal'tsova N.M., Yantsevich A.A.: 2001, *Radiophys. Radioastron.*, **6**, 252.

Boev A.G.: 2005, *Radiophys. Radioastron.*, **10**, 367.

Bragynskyi S.I.: 1963, *Questions of plasma theory* (in Russian), **1**, 183, Gos. izdatel'stvo literature po nauke i tekhnike/eds. Leontovich M.A., Moscow.

Dessler A.J., Hill T.V.: 1979, *ApJ*, **227**, 664.

Flag R.S., Greenman W.B., Reyes F., Carr T.D.: 1991, *A Catalog of High Resolution Jovian Decametric Radio Noise Burst Spectra*, **1**, 199, – (University of Florida, Gainesville).

Hess S., Mottez F., Zarka P.: 2007, *JGR*, **112**, A11212.

Genova F.: 1985, *Planetary Radio Emission*, 51-71, Proc. of an international workshop, Graz, Austria, July 9–10, 1984).

Gerard J.C., Bonfond B., Grodent D. et al: 2014, *JGR Sp.Phys.*, **119**, 11, 9072-9088.

Goldreich P., Lynden-Bell B.: 1969, *ApJ*, **156**, 59.

Kadomtsev B.B.: 1963, *Questions of plasma theory* (in Russian), **2**, 132, Gos. izdatel'stvo literature po nauke i tekhnike/eds. Leontovich M.A., Moscow.

Kadomtsev B.B.: 1988, *Collective phenomena in the plasma* (in Russian), 303, Nauka, Glav. red. phys.-mat. literature, Moscow).

Khurana K. K., et al.: 2004, *Jupiter: The Planet, Satellites and Magnetosphere*, Cambridge University Press/eds. Bagenal, Fran, et al.

Leblanc Y., Bagenal F., Dalk J.A.: 1993, *A&A*, **276**, 603.

Liu Z.Y., Zong Q.G., Blanc M. et al.: 2021, *JGR Sp. Phys.*, **126**, 10.1029/2021JA029710.

Marques M.S., Zarka P. et al.: 2017, *A&A*, **604**, A17.

Panchenko M., Rosker S., Rucker H.O. et al.: 2018, *A&A*, **610**, 101.

Ryabov B.P., Gerasimova N.N.: 1990, *Decameter sporadic radioemission of Jupiter* (in Russian), 240, Kyiv: Naukova dumka.

Ryabov V.B.: 2001, *Radiophys. Radioastron.*, **6**, 103.

Ryabov V.B. et al.: 2014, *A&A*, **568**, A53.

Sentman D.D., Allen J.A., Goerts C.K.: 1975, *GeoRL*, **2**, 465.

Smirnov B.M.: 1995, *Physics of the low ionized gas* (in Russian), 424, Nauka, Glav. red. phys.-mat. literature, Moscow.

Su Y.J., Jones S.T., Ergun R.E. et al.: 2006, *JGR*, **111**, A06211.

Tsvyk N.O.: 2019, *OAP*, **32**, 105.

Tsvyk N.O.: 2023, *OAP*, **36**, 145.

Tsvyk N.O.: 2024, *OAP*, **37**, 94.

Withers P., Vogt M.F.: 2017, preprint (arXiv: 1702.07075v1).

Wu C.S.: 1985, *Space Sci. Rev.*, **41**, 215.